ORIGINAL PAPER

The Influence of Temperature on Coumarin 153 Fluorescence Kinetics

Krzysztof Dobek

Abstract The influence of temperature varied in the range 183 K–323 K on the fluorescence quantum yield, fluorescence lifetime, absorption and emission transition moments and non-radiative deactivation rate was determined for the well known and largely used dye Coumarin 153, dissolved in 1-chloropropane. The Kennard-Stepanov relation connecting the absorption and emission spectra was used to check for the presence of more than one absorbing/emitting species and to investigate whether intramolecular vibrational redistribution completes in the C153 excited S_1 state before the emission takes place. The emission spectrum corresponding to $S_1 \rightarrow S_0$ transition, was fitted at each temperature to the model function including the information on the dye vibrational modes coupling. In this way the displacement in equilibrium distance for the most active vibrational mode was determined for C153 in S_1 and in S_0. Using the temperature dependence of the fluorescence decay time and quantum yield, the non-radiative deactivation rate was determined. Its temperature dependence was compared to that calculated using the theoretical model with the most active vibrational mode displacement values taken from steady-state spectra analysis. The somewhat surprising dependence of the fluorescence decay time and quantum yield on temperature was related to non-trivial coupling between low-frequency vibrational modes of C153 in the excited and ground states.

K. Dobek (✉)
Faculty of Physics, Adam Mickiewicz University,
Umultowska 85,
61-614 Poznań, Poland
e-mail: dobas@amu.edu.pl

K. Dobek
Faculty of Physics, Astronomy and Informatics,
Nicolaus Copernicus University,
Toruń, Poland

Introduction

Coumarin 153 (C153, Scheme 1) is a well known dye, probably one of the most often used in fundamental studies of the environment influence on fluorescence properties of a molecule. It is a fairly simple molecule, strongly emissive, which can be used as a perfect model for much more complicated systems. Despite great interest in this molecule, as a representative of a large family of coumarin dyes, its properties, including the intramolecular deactivation, have not been fully recognized yet. This work has been undertaken to establish the temperature influence on C153 absorptive and emissive properties. The dye was dissolved in 1-chloropropane (ClP), a solvent of moderately polarity, widely assumed to interact exclusively non-specifically. Thus, results presented below can serve as a model for the same dye dissolved in other solvents, possibly also for other molecules, like some coumarin derivatives, and most of all it presents a methodology of studying selected temperature dependent effects present in many other dyes.

At room temperature, absorption of light from the C153 ground to the excited electronic state, $S_0 \rightarrow S_1$, is of $\pi\pi^*$ type and connects two electronic states of the two conformers: I, with the julolidine group in *syn* conformation, and II with the same group in *anti* conformation [1, 2]. In supersonic jet conditions the energy difference between the origins of $S_0 \rightarrow S_1$ transition for both conformers is equal only 188 cm^{-1}. In the ground state conformer I seems to be the dominating form, at least in the jet-cooled conditions [1]. The intensity of absorbed light is significant as the

CF$_3$
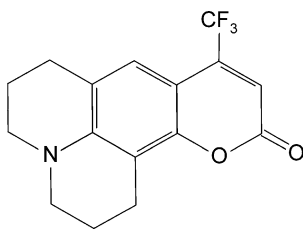
Scheme 1 Coumarin 153 (C153) structure

molecule has a relatively high molar absorption coefficient of ~20,000 lmol^{-1} cm^{-1} [2]. Excitation leads to a change in C153 dipole moment, from 6.6 D to 9.7 D, as derived from thermochromic studies (this parameter's value is still under debate) [3]. This property makes C153 a useful solvatochromic probe, especially for emission studies. In supersonic jet the fluorescence takes place mainly from the excited conformer II [2]. Fluorescence quantum yield of 0.1 in water increases to 0.9 in cyclohexane [4]. Even if in solution the fluorescence activity of both conformers cannot be excluded, their properties must be very similar, as the transition dipole moment for fluorescence has been found to be constant (in the range of experimental error), despite changes in polarity of the environment [5]. Indeed, this similarity has been confirmed by ab-initio calculations in Ref. [6]. The fluorescence decay time fluctuates at room temperature in the range of 4–6 ns in a large set of solvents without any correlation with their polarity [5]. Thus, an increase in the environment polarity, which through solvation leads to a drop in the S_1–S_0 energy gap, results in an increase in non-radiative deactivation, as can be deduced from the influence of environment polarity on quantum yield. These simple properties make C153 so popular, as in most cases the signal resulting from the molecule intramolecular deactivation can be easily separated from the one connected to intermolecular interactions, often quite complicated in nature. Because of a significant change in the dipole moment value, the molecule has been widely used as a solvatochromic [7, 8] or solvation dynamic probe [9–14]. It has been also suggested as an effective probe of its environment hydrogen-bonding-ability [7, 13, 15], a thesis negated by some [16]. In response to its popularity, several attempts at theoretical calculations of the C153 geometry and energy have been undertaken [6, 17]. These works have confirmed the presence of both conformers in the C153 first excited state, reporting them to be almost equal in energy and charge distribution.

At the vibrational level, deactivation of C153 does not look as simply as drawn above. Almost three decades ago Ernsting et al. [18] reported C153 having a surprisingly dense vibronic spectrum of the $\pi\pi^*$ transition. Then, Topp et al. [1] have shown results indicating for the first time the

presence of two C153 conformers and differences in their supersonic-jet fluorescence spectra. Later, Ernsting et al. [2] have shown in supersonic jet that an excitation energy by ≥200 cm^{-1} higher than the conformer I origin transition, lead to an effective intramolecular vibrational redistribution (IVR). The final state of IVR is the excited conformer II, and this is the most important fluorescing species, while a smaller excess in excitation energy leaves the probe in conformer I state. Additionally, the same authors reported that C153 fluorescence decay was most probably controlled by non-trivial vibrational coupling between S_1 and S_0 vibrational states. It was shown that energy exceeding by +44 cm^{-1} and +134 cm^{-1} the conformer I origin excitation energy can lead to an unexpected enhance in oscillator strength in the observed fluorescence of the second and third member of the 132 cm^{-1} vibronic progression, respectively. This result has been connected by Ernsting et al. [2] to mode coupling or Duschinsky rotation. Recently, Eom and Joo [19] reported theoretical normal-mode-projected displacements of C153 25 vibrational modes of frequencies from 25 cm^{-1} to 500 cm^{-1}. Additionally, they provided frequencies of 5 modes visible in the initial 900 fs of the fluorescence decay of C153 in three solvents. Among all these modes, several ones corresponding to 132 cm^{-1} can be found. However, they are not the most active ones. Some, including the low-frequency modes (27 cm^{-1}, 36 cm^{-1}) have been shown to have displacements significantly higher than the modes that can be assumed to correspond to the two most active modes given by Ernsting et al. [2] of lowest frequency. It is not clear, whether these low-frequency modes take part in the molecule deactivation, however one can see that the data reported by Ernsting et al. [2], measured at a resolution of 12 cm^{-1}, could hide a much more complicated picture of C153 deactivation, not attainable with the use of current fluorescence time- or frequency-resolving setups.

This paper shows that non-trivial vibrational mode coupling between S_1 and S_0 C153 vibrational states can influence steady-state fluorescence and decay kinetics in solution at room temperature and below. These results are important as the unusual deactivation of C153 can be erroneously interpreted as an effect of intermolecular interactions. It is the change in temperature that reveals mode coupling, thus especially when used in temperature dependent studies, C153 deactivation should be considered as much more complicated than hitherto assumed.

Steady-state and time-resolved results for C153 dissolved in 1-chloropropane are reported. This system has been already studied by us earlier in Ref. [3], in which it has been shown that the influence of temperature on the emission spectrum position of C153 in five 1-chloroalkanes can be successfully modeled by the McRae continuum solvation model [20]. Ref. [3] presented exclusively the

temperature dependence of steady-state C153 emission spectrum shape and position, examining only the intermolecular solute–solvent interactions. In this work we would like to focus on the influence of temperature on the intramolecular deactivation of C153, and in consequence on the temperature dependence of C153 fluorescence kinetics.

In Ref. [3] a significant change in the shape of the emission spectra with decreasing temperature was reported. This change was assumed to be related to the inhomogeneous broadening of the spectra. Here, on the basis of literature data on C153 vibrational states, the source of the change in shape has been clarified and evaluated. The data obtained from vibronic analysis of the emission spectra allowed an interesting analysis of the non-radiative rate (k_{NR}) of the probe, performed together with experimental time-resolved kinetic results. Fluorescence decays were collected at different temperatures and together with the absorption and emission spectra they were used for determination of the dependence of the fluorescence decay time (τ_F), quantum yield (φ_F), radiative (k_F) and non-radiative rates of C153 in ClP. All these results have thrown new light on the temperature dependence of deactivation of C153 in ClP, and probably also in other weakly interacting solvents. The results presented are important for several reasons: a) they prove the complexity of character of C153 deactivation process, as shown earlier by Ernsting et al. [2] using different experimental methods, b) they show the usefulness of temperature dependent studies of well known dyes, assumed to be almost completely characterized, c) they indicate how much information about the vibrational deactivation can be determined from steady-state absorption/emission spectra in a broad range of temperature in a solvent environment.

Materials and Methods

The chemicals used in the study were the same as in the previous paper [3]. C153 (Fluka) was used as received. 1-chloropropane 99% (ClP, Aldrich), was dehydrated before use over the 3 Å (Merck) and 4 Å (Fluka) molecular sieves. The sample was prepared in argon atmosphere. C153 concentration was kept at the level of 10^{-6}–10^{-5} M.

All measurements were carried using an Oxford Instruments OptistatDN cryostat. Absorption spectra were measured using a Jasco V-550 spectrophotometer adapted to be used with the OptistatDN cryostat. Emission spectra were measured on a home-modernized Aminco SPF-500 spectrofluorimeter with a single photon counting system. The excitation wavelength was set to the maximum of the $S_0 \rightarrow S_1$ absorption band at a selected temperature. Fluorescence quantum yield at room temperature was determined by a relative method using quinine sulfate in 0.1 N H_2SO_4 (φ_F=0.52) as a standard. At other temperatures, using the same C153 in ClP solution, quantum yields were determined by using the φ_F values found at room temperature as reference. Fluorescence decays were collected using a time-correlated single photon counting system (TCSPC) [21]. The excitation wavelength was set to the maximum of the $S_0 \rightarrow S_1$ absorption band at room temperature. This approach was chosen to avoid inevitable changes in excitation pulse shape and in consequence in the instrument response function (IRF), that accompany the changes in the excitation wavelength in our setup. Potential implications of such a decision are discussed at the end of the paper. The decays were collected in 2000 channels. The time per channel was set to 12.2 ps and the scattered signal of Ludox in water solution was used as the IRF of the TCSPC system. The full width at half of the IRF maximum (fwhm) was ~30 ps (measured with a 0.61 ps per channel time resolution). The simplex optimization routine was used in the decay fitting procedure. The decays were collected until 10,000 counts were obtained in the maximum, while the IRF was collected up to 40,000 counts in the maximum.

Calculations

Steady-state Spectra

According to the Kennard-Stepanov relation [22–24], the emission spectrum position and shape can be connected to the absorption spectrum position and shape in the way described by Knox and Sawicki [25]. In short, using the Einstein model of density of the field modes and the relation between the A and B Einstein coefficients, we can define a function of frequency, depending on the absorption and emission spectra of a probe in a homogeneous environment (in MKS [26]):

$$F(v) = \ln\left(\frac{c^2}{8\pi h} \frac{P(v)}{v^3 \sigma(v)}\right) = -\frac{hv}{k_B T} + \frac{hv_0}{k_B T} + \ln\left(\frac{Z}{Z'}\right). \quad (1)$$

$P(v)$ is the emissive power at a selected frequency v, $\sigma(v)$ is the absorption cross section at v, hv_0 is the energy gap between the lowest set of vibrational levels of the electronic states of the probe, S_0 and S_1, Z and Z' are the partition functions for S_0 and S_1. The right side of Eq. 1 can be written as $-\frac{hv}{k_B T} + D(T)$. By taking the derivative of $F(v)$ with respect to v one obtains the formula for the Kennard-Stepanov spectral temperature T*:

$$T^*(v) = -\left[\frac{k_B}{h} \frac{d}{dv} \ln\left(\frac{c^2}{8\pi h} \frac{P(v)}{v^3 \sigma(v)}\right)\right]^{-1}. \quad (2)$$

KS relation predicts a constant $T^*(\nu)$ dependence which up to date, as reported in Ref. [25], has not been found for any experimental system studied. However, $T^*(\nu)$ can give some indications on the number of absorbing/emitting species (manifolds) and the vibronic distribution and relaxation in S_1. The presence of peaks in $T^*(\nu)$ suggest the presence of more then one manifold, whose number can be related to the number of the peaks. Difference between $T^*(\nu)$ and the measured T (usually $T^*(\nu)$ is higher) indicates emission from vibrationally non-relaxed states. Thus, this model has been used to make a preliminary test of the nature of C153 relaxation.

The emission spectra have been also analyzed using the model described in Ref. [27]. On the basis of this model, the emission spectrum of the molecule in a homogeneous non-interacting solvent can be defined as (MKS):

$$I(\nu) = \sum_{n_1} \sum_{n_2} \cdots \sum_{n_N} I_{n_1 n_2 \ldots n_N}(\nu) \tag{3}$$

$$I_{n_1 n_2 \ldots n_N}(\nu) = \left(\frac{E_{00} - \sum\limits_{j=1}^{N} n_j h \overline{\nu}_j}{E_{00}} \right)^3 \prod_{j=1}^{N} \left(\frac{\xi_j^{n_j}}{n_j!} \right)$$

$$\exp \left[-4(\ln(2)) \left(\frac{h\nu - E_{00} + \sum\limits_{j=1}^{N} n_j h \overline{\nu}_j}{\Delta \overline{\nu}_{1/2}} \right)^2 \right] \tag{4}$$

$$\xi_j = 1/2 (\Delta_j)^2 \tag{5}$$

where Δ_j is the change in bond equilibrium distance between the excited and ground states. Note that the third power in Eq. 4 in place of the fourth, as used in Ref. [27], indicates that the emission intensity is given in units of the number of quanta emitted per energy interval [28]. In theory, the model uses all optically active vibrational modes present in the probe molecule. Obviously, the number of modes is truncated to N most active accepting vibrational modes in the ground state. Similarly to $h\nu_0$ in Eq. 1, E_{00} is the energy gap between the lowest levels of the fitted vibronic modes of S_0 and S_1 states. The parameter n_j is the vibronic number of the j-th accepting mode. The summations in Eq. 3 has been limited to small values, high enough to properly model the spectra. The symbol $\overline{\nu}_j$ is the j accepting mode frequency, ν is the frequency at which the emission spectrum is measured, $\Delta \overline{\nu}_{1/2}$ is the full width at half-maximum of the Gaussian inhomogeneous broadening,

and ξ_j is the Huang-Rhys vibrational coupling factor related to the equilibrium bond distance difference between the excited and ground states. Depending on the selected strategy one can try to determine $I_{n_1 n_2 \ldots n_j}(\nu)$ from the quantum mechanically calculated and/or experimentally determined parameter values. The function given in Eq. 3 can also serve as a fitting model. The last approach was chosen in this paper. Several different fitting procedures were tested. Up to three vibrational modes were used. Their frequencies were fitted or fixed to literature values reported by Topp et al. [1], and later by Ernsting et al. [2], given in the experimental section together with the results of the fit. The maximum vibronic number N was varied from 1 to 10. E_{00}, ξ_j, $\Delta \overline{\nu}_{1/2}$ and a scaling a_0 factor (by which $I(\nu)$ was multiplied) were always treated as parameters of the fit. The quality of the fit was estimated using the χ^2 value and the errors of the fitted parameters values.

Kinetic Data

Absorption and emission spectra along with fluorescence decay times and quantum yield values were used for determination of the absorption $|M|^2_{g \to e}$ and emission $|M|^2_{e \to g}$ transition dipole moments modulus squared (CGS) [29].

$$|M|^2_{g \to e} = \frac{1}{n} \frac{2303}{8\pi^3} \frac{3hc}{N_A} \int \frac{\zeta(\nu)}{\nu} d\nu \tag{6}$$

$$|M|^2_{e \to g} = \frac{3h}{64\pi^4} \frac{1}{n^3} k_F \widetilde{\nu}_F^{-3} \tag{7}$$

$$\widetilde{\nu}_F^{-3} = \frac{\int I(\nu) \nu^{-3} d\nu}{\int I(\nu) d\nu} \tag{8}$$

$$k_F = \frac{\varphi_F}{\tau_F}. \tag{9}$$

Above, $\zeta(\nu)$ is the molar extinction coefficient, k_F is the radiative rate constant and $I(\nu)$ is the fluorescence intensity at frequency ν. Time-resolved fluorescence decays were used to determine transition dipole moments but first of all to compare the experimentally determined non-radiative rates with those derived from the Kober et al. model [28]. The rates found experimentally were determined in an ordinary way by using the fluorescence quantum yields and decay times:

$$k_{NR} = \frac{1}{\tau_F} - k_F \tag{10}$$

The model developed in Ref. [28] is a simplified version of the model of the non-radiative deactivation provided by

Jortner, Freed and Englman [30, 31]. In Ref. [30, 31], a constant frequency of the same vibrational modes in the ground and excited electronic state is assumed. The deactivation takes place by transition from the $S_1^{(k)}$ state to the $S_0^{(k)}$ state, which corresponds to a coupling of a ν_k promoting mode in the excited and ground electronic states. Next, the excess energy in S_0 is distributed among the ν_j accepting modes. Assuming the presence of only one, low frequency promoting mode, and one active accepting mode, $\bar{\nu}_A$, the non-radiative decay rate in a homogeneous non-interacting solvent can be defined as (Ref. [28], CGS):

$$k_{NR} = C_k^2 \nu_k \sqrt{\frac{\pi}{2\bar{\nu}_A E_{00}}} \exp(-\xi_A)$$
$$\times \exp\left(-\frac{\gamma E_{00}}{\nu_A} + (\gamma+1)^2 \left(\frac{\Delta\bar{\nu}_{1/2}}{\bar{\nu}_A}\right)^2 / (16\ln(2))\right),$$
(11)

$$\gamma = \ln\left(\frac{E_{00}}{\xi_A \bar{\nu}_A}\right) - 1.$$
(12)

C_k is the electronic coupling between the electronic states participating in the transition through the promoting mode and other parameters are defined as in Eq. 4 (with index $j = A$). The simplifying assumptions used when developing Eq. 11 were as follows: (1) presence of one effective promoting mode, ν_k; (2) no thermal population of the promoting and accepting modes in either the ground or excited state. Clearly, assumption (2) may not be applicable to the data presented in this paper. However, as will be shown, the model gives reasonable qualitative results. As C_k and ν_k are unknown, they have been set to 1, thus the calculations could only be used to check the temperature influence on the rest of Eq. 12. Thus, no direct theoretical (in fact semi-empirical) values of k_{NR} could be reported, but a comparison with the experimental $k_{NR}(T)$ dependence allowed some conclusions on the sources of changes in τ_F and φ_F with temperature as presented in the next section.

Experimental Results

Figure 1 presents C153 absorption $S_0 \rightarrow S_1$ band in 1-chloropropane at different temperatures from the range 183–323 K. Decreasing temperature makes the oscillator strength of the transition mentioned increase. A slight change in the shape and position of the spectrum, bathochromic in character, is also observed.

Obviously, absorption spectra were truncated at a wavelength corresponding to the minimum signal between the $S_0 \rightarrow S_1$ band and the next blue one. Figure 2 presents
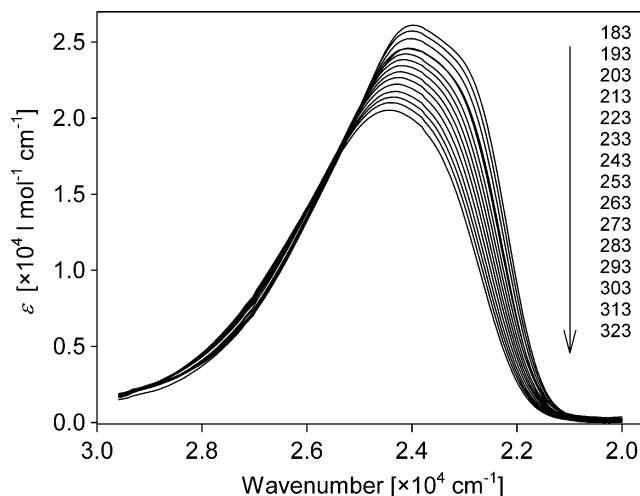

Fig. 1 C153 in ClP absorption spectra

the KS T*(ν) dependencies. T*(ν) was calculated numerically with a derivative window of 10 points. As reported by Sawicki and Knox [25], it has been found that smaller windows lead to the same T*(ν) curve shape but the noise increases with the narrowing window width.

Extending the numerical derivation step (Eq. 2) above 10 did not change T*(ν) significantly. As can be seen in Fig. 2, in some range of frequencies T*(ν) has values equal or slightly smaller than the actual temperature. To check the influence of the noise in $F(\nu)$ on T*(ν), the 4th-order polynomial curves were fitted to $F(\nu)$ and their analytical derivatives were used in T*(ν) determination. Such T*(ν) "noiseless" curves were found very similar to those shown in Fig. 2. T*(ν) dependence shows no peaks or singularities. T*(ν) values seem smaller from the actual temperature by ~10 K. The values found at the lowest temperature reach
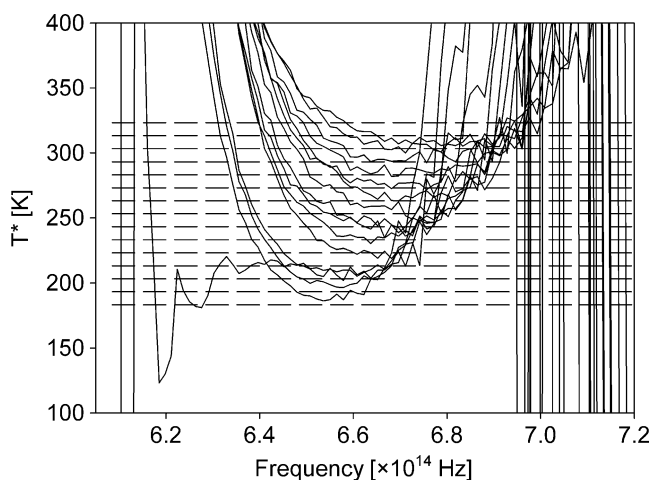

Fig. 2 Kennard-Stepanov T*(ν) dependence zoomed to the region of interest (*dash lines* correspond to subsequent temperatures at which T*(ν) was measured). Statistical error was estimated to be ~10 K

their laboratory counterpart but it is not clear if it is not related to the narrowing of the range in which T*(ν) values are comparable to the actual temperature. Here, it is hard to conclude whether the inequality T*(ν) < T is significant enough to deserve interpretation. The results lead however to an important conclusion that a thermal equilibration of the S_1 C153 state in ClP is reached before fluorescence takes place at each temperature, and no indication of multiple emitting states can be found in the T*(ν) dependence, in accordance to Ref. [5] results.

At first glance, similar standard picture of the C153 emission process has been found as a result of the fit of the function given in Eq. 3 to the emission spectra. Figure 3 presents the spectra and the curves fitted to them at three selected temperatures.

It has been found that the most reliable results, concluded as such on the basis of χ^2 values and errors of the fitted parameters' values, were obtained when using only one accepting vibrational mode, $\overline{\nu}_A$. It held true irrespective of whether the mode frequency was fitted or fixed during the fit. A vibrational progression of $N=5$ was found to be the most suited to recreate the experimental data. The frequency of the active vibrational mode was found to be in the range 1,006–1,174 cm^{-1}. This range corresponds well to the 1,150 cm^{-1} frequency of the mode reported by Ernsting et al. [2] as the most intense in the fluorescence oscillator distribution of jet-cooled C153. Also two next most active vibrational modes, reported by these authors, 810 cm^{-1} and 360 cm^{-1}, were used additionally during the fit, together with the 1,150 cm^{-1} mode. However, their presence has been found to blur the result of the fit, as it led to an increase in the errors of the parameters' values. Thus E_{00}, $\overline{\nu}_A$, $\Delta\overline{\nu}_{1/2}$, ξ_A and a_0 were the parameters of the fit. Table 1 gives the values of these
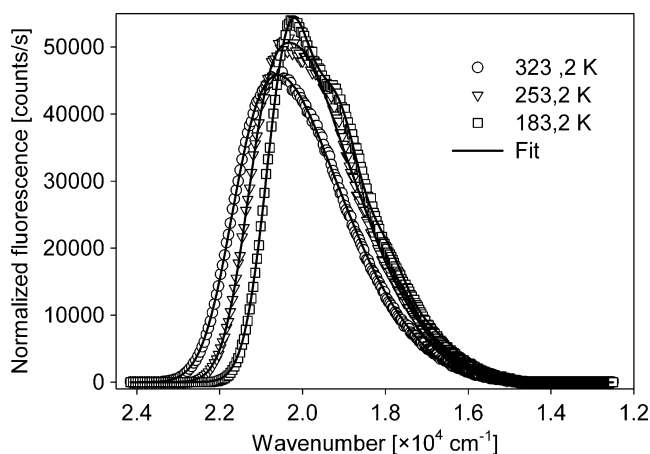
Fig. 3 Experimental emission spectra of C153 in ClP at selected temperatures (323.2 K circles, 253.2 K triangles, 183.2 K squares) and fitted curves of the function given in Eq. 3 (solid line)

parameters at subsequent temperatures set during the experiment.

The values of all parameters correspond quite properly to what should be expected from analysis of Topp et al. [1] and Ernsting et al. [2] works. The latter authors report the three modes mentioned above, 1,150 cm^{-1}, 360 cm^{-1} and 810 cm^{-1}, as the most active together with the fourth mode at 132 cm^{-1}. This last mode has been omitted by them in the modeling of the C153 emission spectra, as the mode subsumed into the broadening function of the 1,150 cm^{-1} mode. The results of the fit reported above indicate that the 1,150 cm^{-1} mode broadening hides also the two other most active vibrational modes in ClP solution, 360 cm^{-1} and 810 cm^{-1}. The displacement of the 1,150 cm^{-1} mode given in Ref. [2] corresponding to ξ_A is slightly smaller than the one given in Table 1. This fact can be related to the difference in the model used in emission simulation, but primarily it is simply connected to the fact that Ernsting et al. studied cooled jet spectra with much better resolved vibrational distribution, in gas phase. A comparison of the results of the fit with $\overline{\nu}_A$ fixed to 1,150 cm^{-1} with those given in Table 1 have shown ξ_A to be correlated with $\Delta\overline{\nu}_{1/2}$. When $\overline{\nu}_A$ is fixed, the only parameter not showing monotonic change with temperature is ξ_A, while it is not the case for the results presented in Table 1. Here $\overline{\nu}_A$ and ξ_A have a common extreme at 293 K, as shown in Fig. 4.

Later it is shown that this effect has physical source and is not simply a result of correlations between fitted parameters. Generally, temperature changes of all parameters given in Table 1 follow the expected way. Due to decreasing energy of the solute–solvent interactions, E_{00} rises with temperature. As observed by Ernsting et al., ξ_A and $\Delta\overline{\nu}_{1/2}$ follow the same temperature dependence as E_{00}. The values of a_0 fall with temperature, which is connected primarily with the drop in absorbance with temperature rising, as shown in Fig. 1. The value of $\Delta\overline{\nu}_{1/2}$ is higher than the values given in Ref. [2], but it is a consequence of a stronger broadening related to solute–solvent interactions taking place in ClP and absent in the gas-phase.

Estimation of the electronic coupling between two singlet states can be made by determining the absorption and emission transition moments, given in Eqs. 6 and 7. To compute $|M|^2_{e \to g}$ the value of k_F was needed (Eq. 9). Thus, the fluorescence decay time, τ_F, and fluorescence quantum yield, φ_F, were determined. Figure 5 shows temperature dependencies of both quantities.

As can be seen, the values of τ_F and φ_F cannot be interpreted in the same simple way as the data reported earlier in this work. It must be stressed that the values of both parameters were determined using different setups, φ_F with Jasco V-550 and Aminco SPF-500 spectrometers, while τ_F with the TCSPC system. The only common part was the cryostat and the object of study. The sample was

Table 1 E_{00}, $\overline{v}_A$, $\Delta\overline{v}_{1/2}$, ξ_A and a_0 values obtained as a result of the fit of the function given in Eq. 3 to the emission spectra of C153 in ClP measured at selected temperatures

T [K]	E_{00} [cm^{-1}]	$\Delta\overline{v}_{1/2}$ [cm^{-1}]	$\overline{v}_A$ [cm^{-1}]	ξ_A	a_0
323	22,210±50	1,570±10	1,030±10	2,14±0,02	16,850±300
313	22,170	1,535	1,025	2,13	17,340
303	22,120	1,495	1,010	2,17	17,230
293	22,100	1,445	1,005	2,24	16,920
283	22,015	1,440	1,020	2,15	19,130
273	21,970	1,410	1,010	2,16	19,810
263	21,920	1,390	1,015	2,15	19,900
253	21,830	1,385	1,025	2,10	21,180
243	21,810	1,360	1,060	2,03	23,050
233	21,730	1,345	1,045	2,02	23,450
223	21,710	1,340	1,090	1,94	25,920
213	21,640	1,320	1,070	1,93	26,070
203	21,630	1,310	1,125	1,83	29,630
193	21,570	1,300	1,165	1,76	33,530
183	21,500	1,290	1,175	1,72±0,01[a]	34,360

[a] A decrease of the error at low temperatures was observed

prepared separately for determination of $\tau_F(T)$ and $\varphi_F(T)$. We can exclude erroneous operation of the cryostat, as measurements of $\tau_F(T)$ in hexafluoroisopropanol and trifluoroethanol showed a simple monotonic change in τ_F with temperature. On the other hand, in propionitrile the values of τ_F similar to those shown in Fig. 5 were observed. These results will be presented elsewhere, here it should be noted that the two protic solvents can form strong hydrogen bonds while propionitrile cannot, therefore such differences in $\tau_F(T)$ are possible. Discontinuous changes in temperature dependences are typical of phase-transition phenomena. It is most probable that a phase-transition in ClP would lead to visible changes in the absorption and especially in the emission spectra of C153. For instance, such observation was made by the author for 4-aminopthalimide dissolved in 1-chloroalkanes not properly dehydrated. As no such changes were observed it was assumed that the surprising

$\tau_F(T)$ and $\varphi_F(T)$ dependencies must be related to some intra-molecular changes in the deactivation process controlled by temperature. However, the abrupt change in the character of the dependence is most probably only related to the small temperature resolution of the experiment. These results lead to k_F and k_{NR} (Eq. 10) values presented in Fig. 6; k_F is approximately three times higher than k_{NR}. There are two temperatures at which drastic changes in $k_F(T)$ and $k_{NR}(T)$ take place: 270 K and 300 K. These changes take place in the temperature range at which only the changes in $\xi_A(T)$ and $\overline{v}_A(T)$ are observed (Fig. 4). The ratio of the minimal vs maximal k_F equals only 0.97, while for k_{NR} this ratio is 0.75. However, because of higher values of k_F the absolute change in k_{NR} is only about twice as big as that in k_F.

With $k_F(T)$ determined, the emissive transition moment, $M_{e\rightarrow g}$, was calculated along with the absorption one, $M_{g\rightarrow e}$.
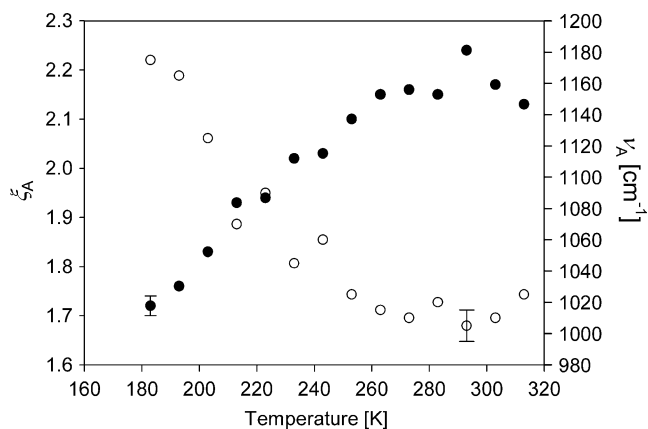
Fig. 4 Temperature dependence of the accepting mode displacement (ξ_A, *filled circles*) and frequency ($\overline{v}_A$, *empty circles*) as obtained from fit of C153 emission spectra to the model given in Eqs. 3–5
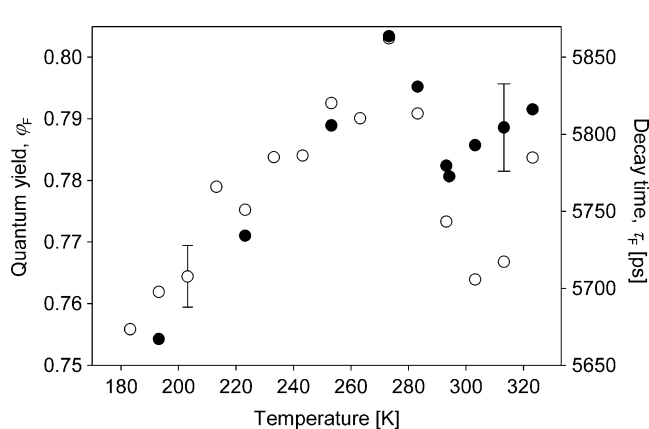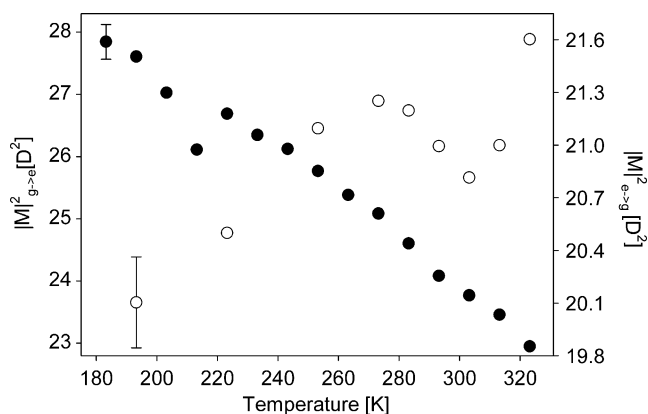

Fig. 5 Fluorescence decay time (*filled circles*) and quantum yield (*empty circles*) vs temperature. *Vertical lines* indicate estimated errors of the values of the corresponding parameters
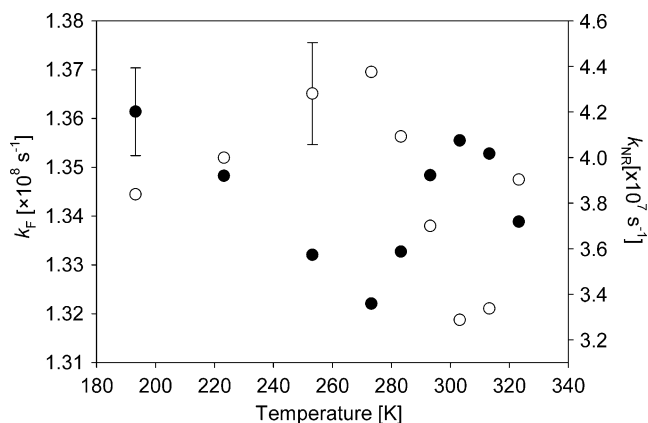
Fig. 6 Radiative (*empty circles*) and non-radiative (*filled circles*) rates vs temperature. *Vertical lines* indicate estimated errors of the corresponding values of the parameters

Figure 7 presents the temperature dependencies of these quantities modulus squared, indicating the probability of absorption and emission as functions of temperature.

The values are similar to the ones reported in Ref. [5]. In accordance to what could be concluded from the changes in signal intensity in the absorption spectra (Fig. 1), reducing temperature leads to a rise in the absorption probability. The dependence is monotonic (disregarding one clearly errone-ous point). Thus, the $M_{g\rightarrow e}(T)$ dependence is quite ordinary and can be connected to a drop in the $S_0 \rightarrow S_1$ energy gap with decreasing temperature. The $M_{e\rightarrow g}(T)$ dependence follows the dependence of $k_F(T)$. Nevertheless, the change in $M_{g\rightarrow e}$ is an order of magnitude larger than that in $M_{e\rightarrow g}$. Now, an attempt to model the temperature dependence of k_{NR} was made. Figure 8 presents $k_{NR}(T)$ obtained with Eq. 11, assuming $C_k = \nu_k = 1$, and once again experimental $k_{NR}(T)$ is shown, for the sake of comparison. Arbitrary units are used in the figure to underline the relativity of the k_{NR} theoretical values.


Fig. 7 Absorption (*filled circles*) and emission (*empty circles*) modulus squared of the transition dipole moments. *Vertical lines* indicate estimated errors of the values of the corresponding parameters
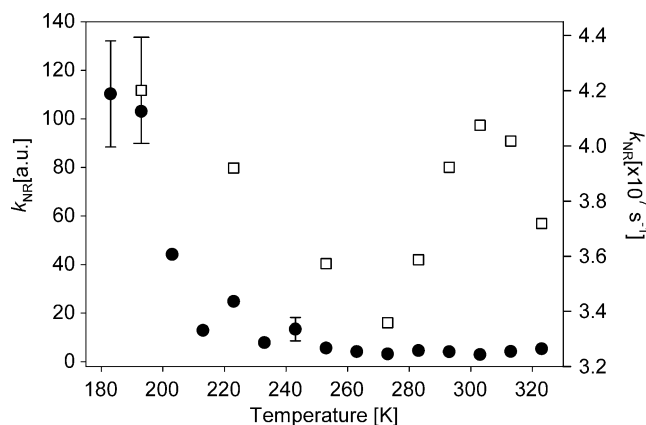
Fig. 8 Non-radiative deactivation rate for C153 in ClP at different temperatures determined using Eq. 11 (*filled circles*, left axis) and Eq. 10 (*empty squares*, right axis). Electronic coupling term, C_K, and promoting mode, ν_k, are assumed to be equal 1. Estimated errors of the values were found to be of the order of the values, see details in the text

At T≤273 K, k_{NR} determined in both ways falls with rising temperature. As far as the theoretical k_{NR} is concerned, the temperature dependence corresponds well to what could be expected from the non-radiative deactiva-tion energy-gap law. To evaluate the $C_k^2 \cdot \nu_k$ term of Eq. 11, assumed until now to be equal 1, the experimental k_{NR} (Eq. 10) has been divided by the theoretical one (Eq. 11). Figure 9 presents this relation.

The $C_k^2 \cdot \nu_k$ temperature dependence indicates a signifi-cant change in the coupling between promoting mode vibrational states in S_1 and S_0. It can also be related to a change in the main active promoting mode or both. Finally, one cannot exclude the erroneousness of the assumption of the presence of a single promoting mode taken to use Eq. 11 to evaluate k_{NR}.
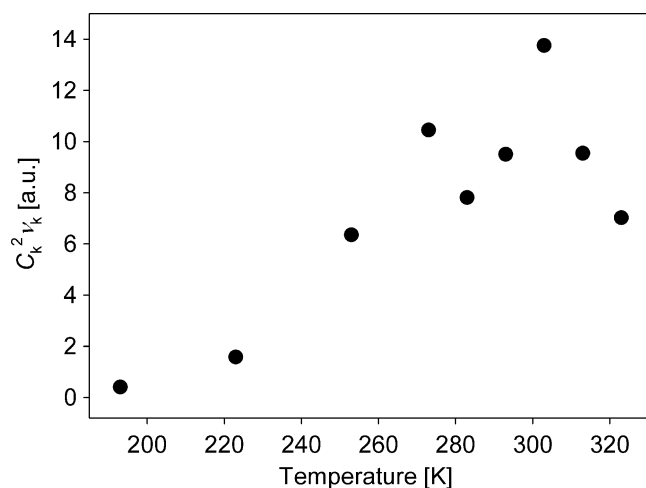
Fig. 9 Temperature dependence of the $C_k^2 \cdot \nu_k = \frac{k_{NR}^{exp}}{k_{NR}^{theor}}$ ratio, k_{NR}^{exp} being the non-radiative deactivation rate determined from Eq. 10 and k_{theor}^{exp} the same determined from Eq. 11

Discussion

Changes in k_F and $M_{e \to g}$ with temperature clearly indicate a non-trivial change in electronic coupling between the optically active vibrational modes in S_1 and S_0. For $M_{g \to e}(T)$ it is the opposite, the dependence is classical. If assuming, as in Ref. [2], conformer I to be the species active in absorption, one could relate the $M_{e \to g}(T)$ dependence to the barrier activated conformational change in C153 from conformer I to II. However, such an interpretation is not supported by the gas-phase results [2], and should lead to a much simpler $k_{NR}(T)$ dependence (Fig. 8). As mentioned above, the 1,150 cm^{-1} mode was assumed to cover, due to inhomogeneous broadening, the non-trivial 132 cm^{-1} mode revealed in Refs [1, 2]. For this low-frequency mode the assumption of the absence of thermal occupation in S_1, taken when using Eqs. 3 and 11, is certainly wrong. As Ernsting et al. [2] found the optical activity of this mode be strongly dependent on the excitation light energy, it can be concluded that its temperature dependent occupation may lead to some untypical results like the one reported in this paper. As mentioned in the introduction section, Eom and Joo [19] reported the low-frequency modes (at 27 cm^{-1}, 36 cm^{-1}) with displacements significantly greater than that of the 132 cm^{-1} mode. Although, we do not know if these modes are visible, it is possible that the 1,150 cm^{-1} mode covers not only the 800 cm^{-1}, 360 cm^{-1} and 132 cm^{-1} ones but also some other ones, during the steady-state emission spectra fit as carried out in this work. Thus, temperature most likely affects the coupling of several modes which together give the 1,150 cm^{-1} response as observed above. As one of low-frequency modes is highly likely to be the promoting one, it is not surprising to see that temperature affects non-trivially not only the emission (Figs. 3, 4 and 5), but also the non-radiative deactivation process (Figs. 6, 8 and 9). It is however not possible, on the basis of the results presented in this paper, to indicate which modes are the responsible for the change in coupling with temperature as shown by the fluorescence deactivation.

It is worth noting that while it is hard to find a temperature dependence of any of the fitted parameters given in Table 1 similar to those shown for τ_F and φ_F in Fig. 5, a reconstruction of the C153 emission spectra based on Table 1 values led to a $\varphi_F(T)$ dependence very similar to the experimental one. It indicates the correctness of the emission spectra fits. The only manifestation of the non-trivial $\tau_F(T)$ and $\varphi_F(T)$ dependencies in the fits is the change in the character of $\bar{\nu}_A(T)$ and $\xi_A(T)$ dependencies at T>273 K (Fig. 4), that is in the same temperature range in which the most abrupt changes in $\tau_F(T)$, $\varphi_F(T)$, $k_F(T)$, $k_{NR}(T)$ and $M_{e \to g}(T)$ take place. It seems that the $\xi_A(T)$ dependence does not undergo important changes in shape,

because the $\bar{\nu}_A$ vibrational mode fitted to the emission spectrum is an average mode incorporating the 1,150 cm^{-1} mode as well as the 132 cm^{-1} one, or even lower-frequency modes. The low-frequency modes are the one found in the supersonic-jet fluorescence studies to undergo strange coupling, while the 1,150 cm^{-1} mode was not found to behave non-classically. Reassuming, fits to the model given by Eqs. 3–5 have shown that the dominating vibrational mode taking part in the fluorescence can hide lower-frequency modes responsible for a non-monotonic character of the $\tau_F(T)$ and $\varphi_F(T)$ dependencies. This inevitably leads also to the smooth theoretical $k_{NR}(T)$ dependence shown in Fig. 8, which results in the $C_k^2 \cdot \nu_k$ temperature dependence (Fig. 9).

Taking into account the scale of different rate constants and the $C_k^2 \cdot \nu_k$ temperature dependence one can finish the analysis with the following conclusion: the non-trivial deactivation a) is mainly manifested in the radiative rate, k_F, b) is also observed in the promoting mode coupling, through which it influences the non-radiative rate, k_{NR}, c) is not observed in the high-frequency vibrational mode coupling, d) is most probably related to temperature dependent vibronic distribution of the low-frequency modes. Unfortunately, the reason for the non-trivial coupling remains unclear, as well as the promoting mode activity.

As fluorescence decays were collected after excitation of C153 at the wavelength corresponding to the absorption maximum at room temperature, while the emission spectra after excitation at the wavelength set to the actual temperature absorption maximum, we have to consider possible implications of this approach on the results. Excitation wavelength was changed in the range 409 nm–417 nm. This range is not wide, similarly as the difference in absorption at a selected temperature at the wavelength corresponding to the absorption maximum and at the wavelength corresponding to the maximum at room temperature. As mentioned above, absorption measurements reflected a very simple image of C153 $S_0 \to S_1$ transition. On the other hand, steady-state fluorescence spectra revealed an unusual behavior, exactly the same as the one found for the fluorescence decay time. It indicates that IVR leads to the same C153 vibrational configuration, despite little differences in excitation energy. Additionally, it is consistent with the picture drawn in Ref. [2]. Although, it can be assumed that the procedure selected during the experiment did not influence the overall effect observed.

At the end it should be reminded that in Ref. [2] the authors discussed the possibility of the presence of a proximity effect, as a result of a low lying S_2 state. Such an effect could in principle affect the coupling between vibronic modes, depending on temperature and excitation energy, which in the case of the fluorescence measurements

was growing with decreasing temperature, due to the bathochromic shift of the absorption spectrum. However, as Ernsting et al. and later Cave and Castner [6] have shown, the S_2–S_1 difference is in the range 0.3 eV–0.8 eV, so it seems to be too large to allow any proximity effect to occur.

Conclusions

The absorption of light by C153 in ClP has been shown to be an ordinary process, growing in probability with decreasing temperature of the solution. The absorption spectra together with the emission spectra could be related in a satisfying way through the Kennard-Stepanov relation. This analysis indicated that a single electronic species absorbs the light as well as a single species emits the light. This result is in accordance with Ernsting et al. [2] observation that conformer I is the absorbing one, while conformer II is the emitting one.

Kinetic results did not show such a simple picture of C153 deactivation behavior. The fluorescence decay time, quantum yield and transition moment were found to change abruptly twice with decreasing temperature. This observation was related mainly to significant and abrupt temperature changes in the radiative deactivation rate of electronically excited C153. Low-frequency vibrational modes, one of them reported earlier in literature as showing unordinary behavior, were proposed as responsible for the observed strange deactivation temperature dependence.

References

1. Pryor BA, Palmer PM, Chen Y, Topp MR (1999) Identification of dual conformers of Coumarin 153 under jet-cooled conditions. Chem Phys Lett 299(6):536–544
2. Mühlpfordt A, Schanz R, Ernsting NP, Farztdinov V, Grimme S (1999) Coumarin 153 in the gas phase: optical spectra and quantum chemical calculations. Phys Chem Chem Phys 1:3209–3218
3. Tomczak J, Dobek K (2009) Coumarin 153 emission thermochromism studied in non-specifically and specifically interacting solvents. J Luminescence 129(8):884–891
4. Jones G II, Jackson WR, Choi C-Y, Bergmark WR (1985) Solvent effects on emission yield and lifetime for coumarin laser dyes.

5. Lewis JE, Maroncelli M (1998) On the (uninteresting) dependence of the absorption and emission transition moments of coumarin 153 in solvents. Chem Phys Lett 282(2):197–203
6. Cave RJ, Castner EW Jr (2002) Time-dependent density functional theory investigation of the ground and excited states of coumarins 102, 152, 153, and 343. J Phys Chem A 106 (50):12117–12123
7. Królicki R, Jarzęba W, Mostafavi M, Lampre I (2002) Preferential solvation of coumarin 153—the role of hydrogen bonding. J Phys Chem A 106(9):1708–1713
8. Molotsky T, Huppert D (2002) Solvation statics and dynamics of coumarin 153 in hexane-propionitrile solvent mixtures. J Phys Chem A 106(37):8525–8530
9. Maroncelli M, Fleming GR (1987) Picosecond solvation dynamics of coumarin 153: the importance of molecular aspects of solvation. J Chem Phys 86(11):6221–6239
10. Bart E, Meltsin A, Huppert D (1994) Solvation dynamics of coumarin 153 in molten salts. J Phys Chem 98(13):3295–3299
11. Chapman CF, Fee RS, Maroncelli M (1995) Measurements of the solute dependence of solvation dynamics in l-propanol: the role of specific hydrogen-bonding interactions. J Phys Chem 99 (13):4811–4819
12. Kovalenko SA, Ruthman J, Ernsting NP (1997) Ultrafast stokes shift and excited-state transient absorption of coumarin 153 in solution. Chem Phys Lett 271(1–3):40–50
13. Gustavsson T, Cassara L, Gulbinas V, Gurzadyan G, Mialocq J-C, Pommeret S, Sorgius M, van der Meulen P (1998) Femtosecond spectroscopic study of relaxation processes of three amino-substituted coumarin dyes in methanol and dimethyl sulfoxide. J Phys Chem A 102(23):4229–4245
14. Karmakar R, Samanta A (2002) Solvation dynamics of coumarin-153 in a room-temperature ionic liquid. J Phys Chem A 106 (18):4447–4452
15. Ito N, Kajimoto O, Hara K (2002) High-pressure studies of rotational dynamics for coumarin 153 in alcohols and alkanes. J Phys Chem A 106(25):6024–6029
16. Horng ML, Gardecki JA, Papazyan A, Maroncelli M (1995) Subpicosecond measurements of polar solvation dynamics: coumarin 153 revisited. J Phys Chem 99(48):17311–17337
17. Ingrosso F, Ladanyi BM, Mennucci B, Elola MD, Tomasi J (2005) Solvation dynamics in acetonitrile: a study incorporating solute electronic response and nuclear relaxation. J Phys Chem B 109 (8):3553–3564
18. Ernsting NP, Asimov M, Schäfer FP (1982) The electronic origin of the ππ* absorption of amino coumarins studied in a supersonically cooled free jet. Chem Phys Lett 91(3):231–235
19. Eom I, Joo T (2009) Polar solvation dynamics of coumarin 153 by ultrafast time-resolved fluorescence. J Chem Phys 131 (24):244507
20. McRae EG (1957) Theory of solvent effects on molecular electronic spectra. Frequency shifts. J Phys Chem 61(5):562–572
21. Karolczak J, Komar D, Kubicki J, Wróżowa T, Dobek K, Ciesielska B, Maciejewski A (2001) The measurements of pcosecond fluorescence lifetimes with high accuracy and subpicosecond precision. Chem Phys Lett 344(1–2):154–164
22. Kennard EH (1918) On the thermodynamics of fluorescence. Phys Rev 11(1):29–38
23. Kennard EH (1926) On the interaction of radiation with matter and on fluorescent exciting power. Phys Rev 28 (4):672–683
24. Stepanov BI (1957) Универсальное соотношение между спет - рами поглощения и люминесценции сложных молекул. Dokl Akad Nauk SSSR 112:839

Requirements for a rotatory decay mechanism. J Phys Chem 89 (2):294–300

25. Sawicki AD, Knox RS (1996) Universal relationship between optical emission and absorption of complex systems: an alternative approach. Phys Rev A 54(6):4837–4841
26. Depending on the unit system most frequently used in the literature presenting cited in the paper equations, CGS or MKS units are used in the paper, as marked in the text
27. Caspar JV, Westmoreland TD, Allen GH, Bradley PG, Meyer TJ, Woodruff WH (1984) Molecular and electronic structure in the metal-to-ligand charge-transfer excited states of d6 transition-metal complexes in solution. J Am Chem Soc 106 (12):3492–3500
28. Kober EM, Caspar JV, Lumpkin RS, Meyer T (1986) Application of the energy gap law to excited-state decay of osmium(II)-polypyridine complexes: calculation of relative nonradiative decay rates from emission spectral profiles. J Phys Chem 90(16):3722–3734
29. Birks JB (1970) Photophysics of aromatic molecules. Wiley-Interscience, New York
30. Englman R, Jortner J (1970) The energy gap law for radiationless transitions in large molecules. Mol Phys 18(2):145–164
31. Freed KF, Jortner J (1970) Multiphonon processes in the nonradiative decay of large molecules. J Chem Phys 52(12):6272–6292